Brief Communication

Low Voltage-Activated Ca^{2+} Channels Are Coupled to Ca^{2+}-Induced Ca^{2+} Release in Rat Thalamic Midline Neurons

Trevor A. Richter, Miloslav Kolaj, and Leo P. Renaud
Neurosciences, Ottawa Health Research Institute, Ottawa, Ontario, Canada K1Y 4E9

High voltage-activated Ca^{2+} channels are coupled to the release of Ca^{2+} from intracellular stores. Here we present evidence that, in the paraventricular thalamic nucleus and other midline thalamic nuclei, activation of low voltage-activated (LVA) Ca^{2+} channels stimulates Ca^{2+}-induced Ca^{2+} release (CICR) from intracellular stores. Voltage-clamp activation of LVA Ca^{2+} channels in fluo-4 AM-loaded neurons induced an initial transient increase in intracellular Ca^{2+} concentrations ($[Ca^{2+}]_i$) (mean increase, 19.4%; decay time constant, 71 ms) that reflected the entry of extracellular Ca^{2+}. This was followed by a sustained secondary elevation in $[Ca^{2+}]_i$ (mean increase, 4.7%; decay time constant, 7310 ms) that was attributable to CICR. Repeated activation of LVA Ca^{2+} channels to evoke CICR caused a progressive buildup of baseline $[Ca^{2+}]_i$ (mean increase, 13.12 ± 3.41%) that was reduced by depletion of intracellular Ca^{2+} stores with thapsigargin or caffeine. In contrast, LVA Ca^{2+} channel-evoked CICR was absent from ventrolateral thalamocortical relay neurons, suggesting that LVA Ca^{2+} channel coupling to Ca^{2+}-dependent intracellular signaling may be a property that is unique to nonspecific and midline thalamocortical neurons.

Key words: **calcium; thalamus; phasic; Ca^{2+}-induced Ca^{2+} release; imaging; neuron**

Introduction

Thalamocortical neurons relay information about external stimuli to primary sensory cortices and exhibit distinct patterns of activity over the sleep–wake cycle, namely tonic firing during wakefulness and phasic bursting and oscillations during slow-wave sleep (Steriade and Timofeev, 2003). Phasic firing is thought to be mediated by the entry of extracellular Ca^{2+} ions via low voltage-activated (LVA) Ca^{2+} channels (Huguenard, 1996; Fuentealba et al., 2004). LVA Ca^{2+} channels (also known as T-type Ca^{2+} channels) typically are activated by depolarization from relatively hyperpolarized membrane potentials (Perez-Reyes, 2003). Although Ca^{2+} entry via LVA Ca^{2+} channels is a central component of intracellular signaling and phasic firing in thalamic neurons, LVA Ca^{2+} channels do not appear to couple to Ca^{2+}-induced Ca^{2+} release (CICR) in specific thalamocortical relay neurons (Budde et al., 2000). To address whether this is characteristic of other thalamic nuclei, including so-called nonspecific intralaminar nuclei, we investigated whether LVA Ca^{2+} channels were coupled to CICR in neurons of the paraventricular nucleus of the thalamus (PVT) and other midline neurons associated with the nonspecific intralaminar thalamocortical system. We observed that activation of LVA Ca^{2+} channels in these midline neurons caused the release of Ca^{2+} from intracellular stores, whereas this feature was generally absent from neurons in specific thalamocortical relay nuclei.

Received May 16, 2005; revised July 26, 2005; accepted July 27, 2005.
This work was supported by Canadian Institutes of Health Research Grant FRN 38022.
Correspondence should be addressed to Dr. Leo Renaud, Neurosciences, Ottawa Health Research Institute, 725 Parkdale Avenue, Ottawa, Ontario, Canada K1Y 4E9. E-mail: lprenaud@ohri.ca.
DOI:10.1523/JNEUROSCI.1942-05.2005
 0270-6474/05/258267-05$15.00/0

Materials and Methods

Slice preparation, electrophysiology, and Ca^{2+} imaging. Experiments performed on Wistar rats (10–25 d of age) conformed to Canadian Council for Animal Care and Ottawa Health Research Institute guidelines for the ethical use of animals in research. Coronal slices of thalamus (300–350 μm) were cut with a vibrating blade microtome (VT1000S; Leica, Nussloch, Germany) and were kept for >1 h in oxygenated (95% O_2/5% CO_2) standard artificial CSF (ACSF) containing the following (in mM): 127 NaCl, 3.1 KCl, 1.3 $MgCl_2$, 2.4 $CaCl_2$, 26 $NaHCO_3$, and 10 glucose, pH 7.3, 300–310 mOsm. Slices were transferred to a recording chamber mounted on a confocal laser-scanning microscope (Zeiss Axioscope 2FS; Carl Zeiss Canada, Toronto, Ontario, Canada) and were perfused continuously at 19–23°C with oxygenated ACSF. For electrophysiological recordings, we used borosilicate thin-walled micropipettes filled with the following (in mM): 130 K-gluconate, 10 KCl, 10 NaCl, 2 $MgCl_2$, 10 HEPES, 1 EGTA, 2 Mg-ATP, and 0.3 Na-GTP, pH adjusted to 7.3 with KOH (pipette resistance, 9–12 MΩ). Data from whole-cell current-clamp and voltage-clamp recordings were obtained with a MultiClamp 700A amplifier (Molecular Devices, Union City, CA), filtered at 1 kHz, and stored on a computer hard drive for off-line analysis. Series resistance was compensated (70–80%) electronically. Leakage currents were not subtracted. Data were not adjusted for liquid junction potential. A Digidata 1322A interface and pClamp 9 software (Molecular Devices) were used on-line to generate current and voltage commands. The inward Ca^{2+} current (I_T) caused by activation of LVA Ca^{2+} channels was recorded in voltage-clamp mode in the presence of tetrodotoxin (TTX; 1 μM; Alamone Labs, Jerusalem, Israel) from cells held at a command potential (V_h) of –50 mV (see Fig. 1*B*). The mean resting membrane potential was –49.9 ± 2.0 mV, and conductance was 0.9 ± 0.1 nS (n = 56). LVA Ca^{2+} channels were activated selectively by transiently hyperpolarizing the cell to –100 mV for 300–1000 ms, followed by a return to the holding potential. We analyzed responses to injections of hyperpolarizing current pulses to monitor changes in membrane conductance.

Individual cells were loaded via the patch pipette with the Ca^{2+}-sensitive dye fluo-4 AM (100 μM; Invitrogen Canada, Burlington, On-

tario, Canada), which was allowed to diffuse for 20 min before imaging. Fluo-4 was excited at 488 nm with an argon laser (7.5 mW), and emitted light was bandpass-filtered at 500–530 nm. Image acquisition was controlled via Zeiss LSM 510 software (Carl Zeiss Canada). Images were collected in frame scan mode at a resolution of 128 × 128 pixels at a scan rate of 10 ms/frame. Preliminary experiments established that this acquisition protocol produced minimal photo bleaching and no photo toxicity. Ca^{2+} imaging data are presented as the percentage of change in fluo-4 fluorescence intensity expressed relative to basal fluorescence intensity ($\Delta F/F$).

Drugs. Unless stated otherwise, drugs and reagents were purchased from Sigma (St. Louis, MO). Drugs were stored as 1000× stock solutions at –20°C and were diluted in ACSF immediately before application. Ba^{2+} (2.4 mM) was added to the bath solution by equimolar substitution for Ca^{2+} in standard ACSF. Ca^{2+} was removed from the bath solution by switching from standard ACSF (2.4 mM Ca^{2+}) to nominally Ca^{2+}-free ACSF [extracellular Ca^{2+} concentration ($[Ca^{2+}]_o$) ≈ 0] [containing the following (in mM): 135 NaCl, 3.1 KCl, 1.3 $MgCl_2$, 26 $NaHCO_3$, and 10 glucose, pH 7.3, 300–310 mOsm].

Data analysis and statistics. Electrophysiological recordings were analyzed off-line with Clampfit version 9 (Molecular Devices). Confocal images were analyzed by using NIH Image (developed at the National Institutes of Health; http://rsb.info.nih.gov/nih-image). Regression and statistical analyses were performed by using GraphPad (San Diego, CA) Prism version 4. To compare data from different treatments, we used ANOVA, Kruskal–Wallis nonparametric ANOVA with Dunn's multiple comparison posttest, and Student's paired *t* test as appropriate. We took $p < 0.05$ to be statistically significant.

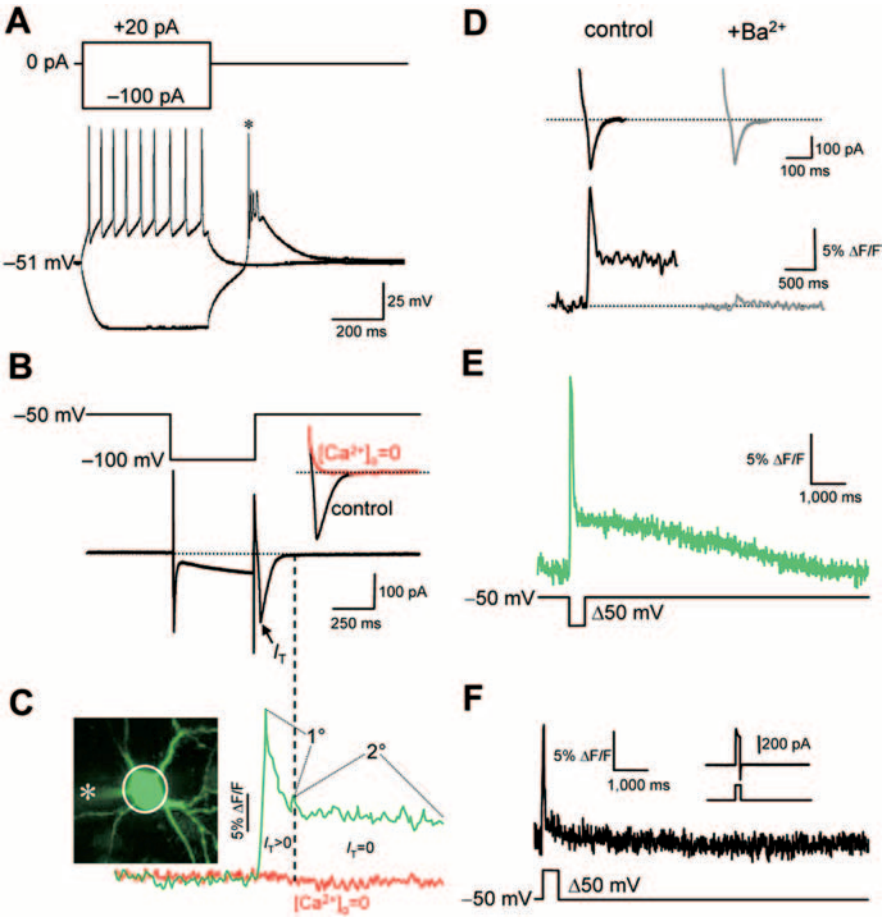

Figure 1. Firing characteristics and Ca^{2+} responses of midline thalamic neurons. ***A***, Current-clamp traces from a representative PVT neuron showing tonic firing (top traces) and a low-threshold spike (bottom trace), which triggers a superimposed Na^+ spike (asterisk). ***B***, Voltage-clamp recording (bottom trace) showing how the activation of LVA Ca^{2+} channels elicits an I_T (bottom trace; arrow). The inset is an example of I_T in the presence (black) and absence (red) of extracellular Ca^{2+}. ***C***, Sample traces of changes in $[Ca^{2+}]_i$ in a representative PVT neuron measured as changes in $\Delta F/F$ of fluo-4. The white circle indicates the area used to measure changes in $[Ca^{2+}]_i$. The green trace corresponds to the current in ***B***. 1° and 2° indicate the primary and secondary phases of the response to which single exponential equations were fit to obtain decay time constants (see Results for details). The red trace is the response of the same cell in nominally Ca^{2+}-free ACSF. The dashed line indicates the time at which I_T returned to zero (***A***, bottom trace). The asterisk indicates the recording pipette. ***D***, Example of the effect of the replacement of extracellular Ca^{2+} with Ba^{2+} (2.4 mM) on I_T (top traces) and the Ca^{2+} response to I_T (bottom traces). All traces were recorded from the same cell and are representative of four cells. Dotted lines indicate baselines. ***E***, Averaged Ca^{2+} responses of 11 PVT neurons (green) to I_T evoked by using the protocol depicted by the black line. ***F***, Averaged Ca^{2+} responses of five PVT neurons ($\Delta F/F$; top trace) to the activation of HVA Ca^{2+} channels, using the protocol depicted by the black line. Inset, Representative trace (top) of current response. Traces in ***B–F*** were recorded in the presence of 1 μM TTX.

Results

PVT and other midline thalamic neurons recorded in current-clamp mode in the absence of TTX exhibited two firing modes. Depolarization from the resting membrane potential (approximately –50 mV) elicited tonic firing (Fig. 1*A*, top traces). In contrast, depolarization that followed transient hyperpolarization (from –50 to –100 mV; 500 ms) elicited a low-threshold Ca^{2+} spike that was crowned with one or more TTX-sensitive Na^+ spikes (Fig. 1*A*, bottom traces). Few PVT neurons (7 of 56) exhibited spontaneous tonic firing.

Ca^{2+} response to activation of LVA Ca^{2+} channels

In voltage-clamp recordings (V_h = –50 mV) obtained in the presence of TTX, the activation of LVA Ca^{2+} channels produced an I_T (mean amplitude, –363.9 ± 49.8 pA; $n = 28$ cells) (Fig. 1*B*, arrow) that was eliminated in nominally Ca^{2+}-free ACSF (I_T reduced by 97.1 ± 2.4% vs control; $p < 0.0001$; $n = 3$) (Fig. 1*B*, inset). Simultaneous recordings in fluo-4-loaded cells revealed a rapid increase in intracellular Ca^{2+} concentrations ($[Ca^{2+}]_i$) in the soma (mean peak $\Delta F/F = 19.40 \pm 5.50\%$; $n = 11$ cells) (Fig. 1*C*, green trace). This elevation in $[Ca^{2+}]_i$ reflected the entry of extracellular Ca^{2+} because (1) the increase in $[Ca^{2+}]_i$ was absent in nominally Ca^{2+}-free ACSF ($\Delta F/F$ reduced by 97.8 ± 2.1% vs control when $[Ca^{2+}]_o \approx 0$; $p < 0.001$; $n = 3$) (Fig. 1*C*, red trace), (2) the amplitude of I_T was correlated with the amplitude of the increase in $[Ca^{2+}]_i$ ($r^2 = 0.93$ for I_T peak vs $\Delta F/F$ peak; $p < 0.001$; $n = 11$), and (3) replacement of extracellular Ca^{2+} with Ba^{2+} (2.4 mM), which did not change the magnitude of I_T significantly (I_T = –451.00 ± 114.05 vs –419.00 ± 110.88 for absence vs presence of Ba^{2+}, respectively; $p > 0.05$; $n = 4$), eliminated the increase in $[Ca^{2+}]_i$ ($\Delta F/F$ reduced by 93.1 ± 2.4% vs control; $p < 0.001$; $n = 4$) (Fig. 1*D*).

The initial peak in $[Ca^{2+}]_i$ (primary phase of the response) (Fig. 1*C*, 1°) decayed rapidly [average decay time constant for single exponential fit between time 0 (I_T peak) and 200 ms, 70.91 ms; $n = 11$], but $[Ca^{2+}]_i$ did not return to baseline at the time expected based on this rate of decay; rather, $\Delta F/F$ decreased rap-

idly to a level that was 4.66 ± 0.79% ($n = 11$) above baseline (~24% of the magnitude of 1°) ~200 ms after the peak in I_T and declined 10-fold slower thereafter (secondary phase of the response; average decay time constant between time 200 and 2000 ms, 7310 ms; $n = 11$) (Fig. 1*C*, 2°). Thus, as exemplified by the green trace in Figure 1*C*, $[Ca^{2+}]_i$ remained elevated after the entry of extracellular Ca^{2+} had ceased ($I_T = 0$) (Fig. 1*C*, right side of dashed line). This secondary phase of elevated $[Ca^{2+}]_i$ usually did not reach baseline by the end of the 2-s-long recording period (Fig. 1*C*, green trace); longer recordings (20 s) revealed that the secondary phase of the Ca^{2+} response lasted for 7.95 ± 1.71 s (range, 1.2–16.7 s) after I_T had decayed to zero ($n = 11$ cells) (Fig. 1*E*).

In five of five PVT neurons tested in the presence of 1 μM TTX, activation of high voltage-activated (HVA) Ca^{2+} channels in voltage-clamp mode via the application of a 500 ms depolarizing pulse (from –50 to 0 mV) (Fig. 1*F*, inset) caused a transient increase in $[Ca^{2+}]_i$ ($\Delta F/F = 15.87 \pm 3.12\%$; $n = 5$) (Fig. 1*F*) that was blocked by 100 μM Cd^{2+} ($\Delta F/F = 0.57 \pm 1.12\%$ in the presence of Cd^{2+}; $p < 0.001$ vs control; $n = 5$). The average time constant for the initial decay phase that followed the transient peak in $[Ca^{2+}]_i$ was 52.01 ms ($n = 5$), which was similar to the time constant of the initial decay phase of the response to activation of LVA Ca^{2+} channels (~71 ms; see above). However, this transient was not followed by a large sustained secondary elevation in $[Ca^{2+}]_i$ such as that in response to the activation of LVA Ca^{2+} channels; in contrast to the ~8-s-long elevation in $[Ca^{2+}]_i$ that followed activation of LVA Ca^{2+} channels (see above) (Fig. 1*E*), $[Ca^{2+}]_i$ decayed to zero within 0.90 ± 0.02 s (range, 0.88–0.96 s) after the activation of HVA Ca^{2+} channels (Fig. 1*F*).

Frequency dependence of LVA Ca^{2+} channel-evoked Ca^{2+} responses

High-frequency stimulation (10 successive hyperpolarizing steps at 1 Hz) (Fig. 2*A*, protocol) caused a progressive increase in $[Ca^{2+}]_i$ that was attributable to a buildup of $[Ca^{2+}]_i$ (mean increase in $\Delta F/F = 13.12 \pm 3.41\%$; $n = 5$) (Fig. 2*A*, bottom, gray trace); this buildup did not occur during low-frequency (0.1 Hz) stimulation (Fig. 2*A*, bottom, black trace; note different time scales). The buildup of $[Ca^{2+}]_i$ was not attributable to changes in I_T, because the magnitude of the 1st and 10th I_T in response to the 10 hyperpolarization steps was the same (mean difference between 1st and 10th I_T, 3.91%; $p > 0.05$ for amplitude of 1st vs 10th I_T; $n = 5$) (Fig. 2*A*, inset).

The buildup of $[Ca^{2+}]_i$ described above was attributable to the activation of LVA Ca^{2+} channels and did not involve HVA Ca^{2+} channels, because 100 μM Cd^{2+} (which blocks HVA Ca^{2+} channels but not LVA Ca^{2+} channels) did not alter the Ca^{2+} response to a 1 Hz series of hyperpolarizing steps (in the absence vs presence of Cd^{2+} $\Delta F/F = 13.1$ vs 13.2%; $p > 0.05$; $n = 5$) (Fig. 2*B*). Moreover, a 1 Hz series of 10 500-ms-long depolarizing steps (from –50 to 0 mV) to activate HVA Ca^{2+} channels (Fig. 2*C*) was associated with transient peaks in $[Ca^{2+}]_i$ but did not cause a buildup of $[Ca^{2+}]_i$ (five of five cells) (Fig. 2*C*, bottom, black trace). These transient peaks in $[Ca^{2+}]_i$ were abolished in the presence of 100 μM Cd^{2+} in five of five cells that were tested (Fig. 2*C*, bottom, gray trace).

Activation of LVA Ca^{2+} channels leads to CICR in PVT neurons

To determine whether the elevated $[Ca^{2+}]_i$ that followed I_T was attributable to the release of Ca^{2+} from intracellular stores, we tested the effects of depleting intracellular Ca^{2+} stores with caffeine or thapsigargin. Application of 10 mM caffeine for 30 s in the absence of any other stimulation caused an elevation in $[Ca^{2+}]_i$ in six of six PVT neurons (mean increase in $\Delta F/F = 14.6 \pm 3.2\%$). This stimulation-independent elevation in $[Ca^{2+}]_i$ (Fig. 3*A*, left inset) reflected the release of Ca^{2+} from intracellular stores, because caffeine application was not associated with any inward current (data not shown). Caffeine caused a decrease in the buildup of $[Ca^{2+}]_i$ that normally occurred during high-frequency stimulation (Fig. 3*A*), as revealed by a significant reduction of the response to the 10th I_T in the series (13.78 ± 3.56%; $p < 0.05$; $n = 6$ cells). This effect was not attributable to a change in the magnitude of I_T, which did not change significantly during the series of 10 I_T during caffeine application ($p > 0.05$; ANOVA; $F = 0.70$; $n = 6$) (Fig. 3*A*, right inset). Moreover, the magnitude of the 10th I_T in the series was the same in the presence of caffeine as in control conditions ($p > 0.05$; $n = 6$) (Fig. 3*A*, right inset).

Thapsigargin (5 μM; ~3 min) did not alter $[Ca^{2+}]_i$ in unstimulated cells (Fig. 3*B*, left inset). However, as with caffeine, the buildup of $[Ca^{2+}]_i$ in response to a high-frequency series of 10 I_T was reduced in the presence of thapsigargin (Fig. 3*B*), as revealed by a 22.13 ± 5.17% decrease in the response to the 10th I_T ($p < 0.05$; $n = 5$ cells). As with caffeine, this effect was not attributable

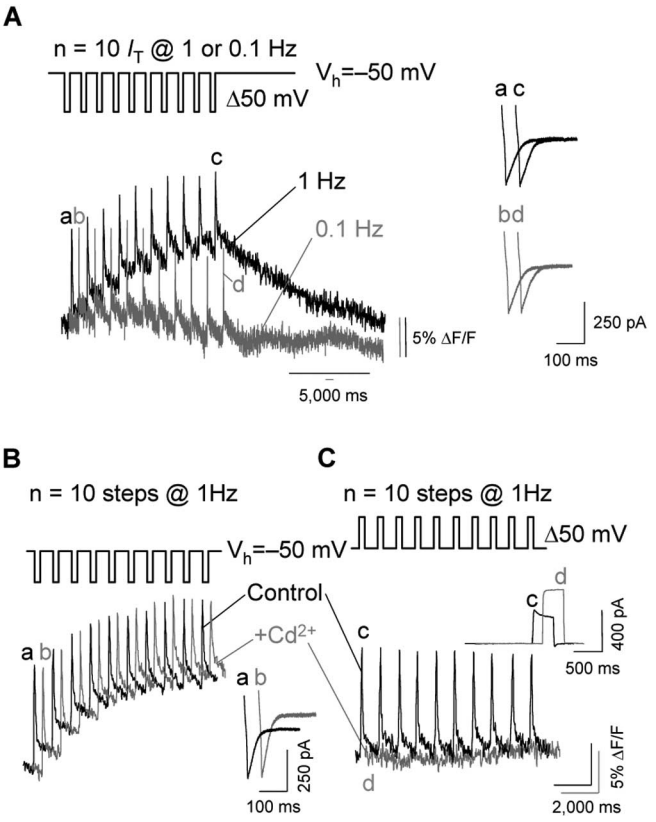

Figure 2. High-frequency activation of LVA Ca^{2+} channels causes a buildup of $[Ca^{2+}]_i$. ***A***, Example of changes in $[Ca^{2+}]_i$ in the same PVT neuron in response to a high-frequency (1 Hz; gray trace) and low-frequency (0.1 Hz; black) activation series of 10 I_T (protocol in top panel). Note the different time scales for the traces. ***B***, Example of changes in $[Ca^{2+}]_i$ in the same PVT neuron in response to a high-frequency (1 Hz) series of 10 I_T (protocol in top panel) in the absence (control; black) and presence (+Cd^{2+}; gray) of 100 μM Cd^{2+}. ***C***, Example of changes in $[Ca^{2+}]_i$ in the same PVT neuron in response to a high-frequency (1 Hz) series of 10 depolarizing pulses (from –50 to 0 mV; protocol in top panel) to activate HVA Ca^{2+} channels in the absence (control; black) and presence (+Cd^{2+}; gray) of 100 μM Cd^{2+}. Insets illustrate current traces for the $\Delta F/F$ responses indicated by the lowercase letters. All traces are offset on the *x*-axis for clarity. Traces in ***A–C*** are representative of five PVT neurons.

to a change in I_T ($p > 0.05$ for amplitude of 1st through 10th I_T; ANOVA; $F = 1.49$; $p > 0.05$ for amplitude of 10th I_T during thapsigargin vs control; $n = 5$ for both) (Fig. 3*B*, right inset).

Distribution of LVA Ca^{2+} channel-evoked CICR within the thalamus

We recorded the Ca^{2+} response to I_T in neurons from several different thalamic nuclei in a separate experiment. Thalamic neurons were classified according to whether they did ($n = 12$) (Fig. 4*A*) or did not ($n = 13$) (Fig. 4*B*) exhibit a buildup of $[Ca^{2+}]_i$ in response to activation of a series of 10 I_T at 1 Hz, which is consistent with CICR. Only cells that exhibited an increase in baseline $[Ca^{2+}]_i$ during the series of I_T also exhibited the secondary phase of elevated $[Ca^{2+}]_i$ (Fig. 4*C*). Moreover, the relative magnitude of the secondary elevation in $[Ca^{2+}]_i$ (ratio of 2° to 1°) was reduced during the series of 10 I_T only in cells that exhibited an increase in baseline $[Ca^{2+}]_i$ ($p < 0.01$ for 2°/1° for Ca^{2+} response to the 1st vs 10th I_T; Kruskal–Wallis nonparametric ANOVA with Dunn's multiple comparison posttest; $n = 25$) (Fig. 4*D*), which likely reflected progressive depletion of intracellular Ca^{2+} stores. Cells that exhibited CICR were located within PVT and midline thalamic nuclei (Fig. 4*E*, black circles). Although CICR was detected in a sample of laterodorsal thalamic nucleus cells, it was consistently absent from cells located within the reticular nucleus and specific thalamocortical nuclei (Fig. 4*E*, gray circles).

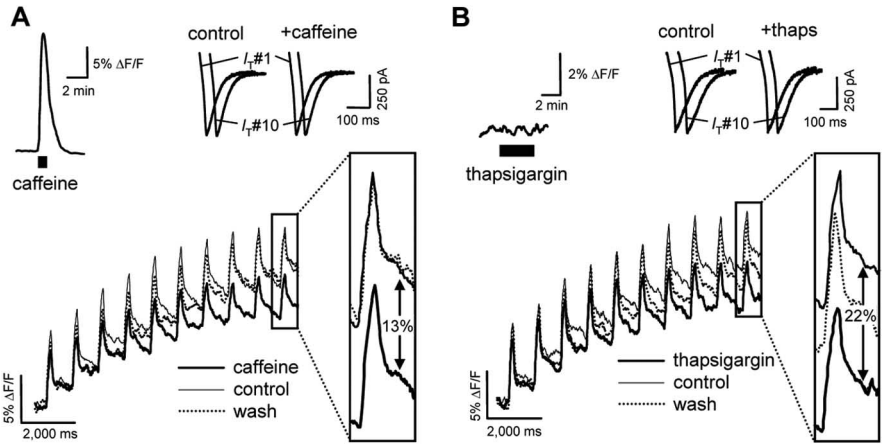

Figure 3. Activation of LVA Ca^{2+} channels evokes CICR in PVT neurons. ***A***, Effect of 10 mM caffeine on buildup of $[Ca^{2+}]_i$ (Fig. 2*A*, top; see protocol). The thick, thin, and dotted lines indicate responses during (<5 min), before (control), and after (wash; 17–21 min) caffeine application, respectively ($n = 6$ cells). The box shows Ca^{2+} responses to the 10th I_T plotted on an expanded scale. The inset at top left shows a representative response to bath application of caffeine. The inset at top right shows average traces ($n = 6$ cells) of the 1st (I_T #1) and 10th (I_T #1) I_T of the series of 10 I_T in the absence (control) and presence of caffeine (+caffeine). ***B***, Effect of 5 μM thapsigargin on buildup of $[Ca^{2+}]_i$. The thick, thin, and dotted lines indicate responses during (<5 min), before (control), and after (wash; 19–26 min) thapsigargin application, respectively ($n = 5$ cells). The box shows Ca^{2+} responses to the 10th I_T plotted on an expanded scale. The inset at top left shows a representative response to bath application of thapsigargin. The inset at top right shows average traces ($n = 5$ cells) of the 1st (I_T #1) and 10th (I_T #10) I_T in the absence (control) and presence of thapsigargin (+thaps). For clarity, traces in ***A*** and ***B*** were smoothed by a rectangular moving average window of width 5 (50 ms); current traces in the right insets in ***A*** and ***B*** are offset on the *x*-axis.

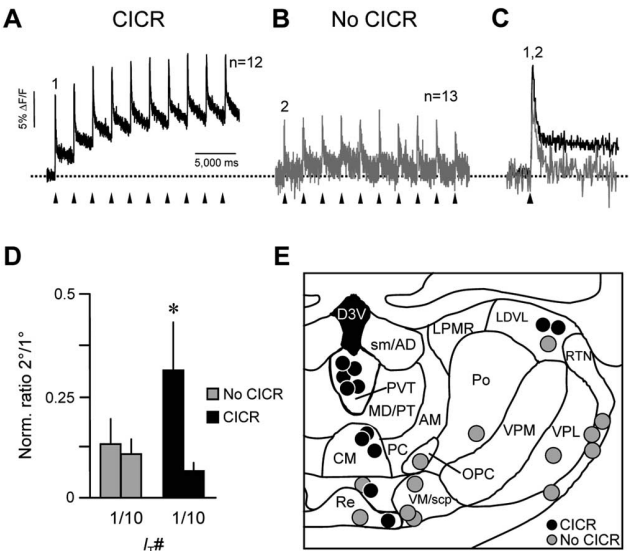

Figure 4. Regional distribution of LVA Ca^{2+} channel-evoked CICR in the thalamus. ***A***, ***B***, Average Ca^{2+} response profiles of thalamic neurons that did ($n = 12$) or did not ($n = 13$) show evidence of CICR (rising baseline) in response to 10 I_T (arrowheads). ***C***, The first Ca^{2+} response in each series in ***A*** and ***B*** (1 and 2, respectively) superimposed on an expanded time scale. Note the absence of the secondary phase of the Ca^{2+} response in the gray trace. ***D***, Normalized mean ± SEM ratio of the secondary phase (2°) relative to the primary phase (1°) of the response for the first (I_T #1) and last (I_T #10) response in a series of 10 I_T. The size of 2° was calculated as the mean value for a 750 ms window from 250 to 1000 ms after the onset of I_T (at 0 ms). Black and gray bars represent cells that did and did not exhibit CICR, respectively (*$p < 0.05$ for normalized ratio 2°/1° in response to I_T #1 vs #10; Kruskal–Wallis nonparametric ANOVA with Dunn's multiple comparison posttest; $n = 25$ cells). ***E***, Distribution of thalamic neurons that exhibited (black circles) or lacked (gray circles) CICR. Data are for the cells in ***A–D***. AM, Anteromedial nucleus; CM, central medial nucleus; LDVL, laterodorsal nucleus, ventrolateral part; LPMR, lateral posterior nucleus, mediorostral part; MD/PT, mediodorsal nucleus, lateral part/paratenial nucleus; OPC, oval paracentral nucleus; PC, paracentral nucleus; Po, posterior thalamic nuclear group; Re, reuniens nucleus; RTN, reticular nucleus; sm/AD, stria medullaris of the thalamus/anterodorsal nucleus; VM/scp, ventromedial nucleus; VPL, ventral posterolateral nucleus; VPM, ventral posteromedial nucleus [based on Paxinos and Watson (1988)].

Discussion

LVA Ca^{2+} channels are crucial for modulating phasic firing in thalamic cells during slow-wave sleep (Fuentealba et al., 2004) and absence epilepsy (Tsakiridou et al., 1995). Activation of these channels normally inhibits tonic firing during sleep (Anderson et al., 2005), as exemplified by the fact that genetic disruption of LVA Ca^{2+} channels in mice causes sleep disturbance because of frequent and prolonged episodes of arousal (Lee et al., 2004; Anderson et al., 2005). Although LVA Ca^{2+} channels do not appear to be coupled to CICR in the dorsolateral geniculate nucleus (dLGN) (Budde et al., 2000), our results indicate that the activation of LVA Ca^{2+} channels evokes CICR in PVT neurons and a selective group of predominantly midline thalamic neurons. This suggests that LVA Ca^{2+} channels may be linked differentially to intracellular signaling pathways in different regions of the thalamus.

The evidence presented here is consistent with the hypothesis that LVA Ca^{2+} channels are coupled to CICR in midline thalamic neurons. The first indication that LVA Ca^{2+} channels might stimulate CICR was the observation that selective activation of these channels, as opposed to HVA Ca^{2+} channels, produced a prolonged elevation in $[Ca^{2+}]_i$ that persisted on average for ~8 s after the initial peak in $[Ca^{2+}]_i$ that was contemporaneous with I_T. Subsequent experiments showed that this prolonged elevation in $[Ca^{2+}]_i$ was attributable to the release of Ca^{2+} from intracellular stores after the initial influx of extracellular Ca^{2+}. Specifically, evocation of a high-frequency series of I_T caused a progressive buildup of $[Ca^{2+}]_i$ without affecting I_T. This buildup was

associated with a decrease in the magnitude of the secondary elevation in $[Ca^{2+}]_i$ as intracellular Ca^{2+} stores were depleted progressively. Moreover, depletion of intracellular Ca^{2+} stores with caffeine or thapsigargin reduced this buildup of $[Ca^{2+}]_i$. Because caffeine and thapsigargin both decrease the release of Ca^{2+} from intracellular stores during CICR, these results are consistent with the hypothesis that activation of LVA Ca^{2+} channels produces CICR. The observation that removal of extracellular Ca^{2+} eliminated the elevation of $[Ca^{2+}]_i$ in response to the activation of LVA Ca^{2+} channels suggested that the release of Ca^{2+} from intracellular stores was initiated by the entry of extracellular Ca^{2+}. In addition, repeated activation (1 Hz) of HVA Ca^{2+} channels failed to cause a buildup of $[Ca^{2+}]_i$, which suggested that the buildup in response to repeated activation of LVA Ca^{2+} channels was specific to these channels and did not involve HVA Ca^{2+} channels. Nevertheless, although the sustained phase of the HVA Ca^{2+} channel-evoked Ca^{2+} response was substantially smaller than that evoked by LVA Ca^{2+} channels, we do not exclude the possibility that HVA Ca^{2+} channels may be coupled to CICR, as is the case in the dLGN (Budde et al., 2000).

Although LVA Ca^{2+} channels do not appear to be coupled to CICR in the dLGN (Budde et al., 2000), these channels are coupled to CICR via caffeine-sensitive ryanodine receptors in midbrain dopaminergic neurons in neonatal rats (Cui et al., 2004). Our finding that LVA Ca^{2+} channels are coupled functionally to CICR in the PVT suggests that LVA Ca^{2+} channels may be coupled differentially to Ca^{2+}-dependent intracellular signaling systems in different regions of the thalamus. Indeed, Ca^{2+} responses that were consistent with CICR were observed predominantly (but not exclusively) in midline nuclei, whereas cells in specific thalamocortical relay nuclei did not exhibit CICR. Interestingly, PVT neurons that exhibited LVA Ca^{2+} channel-evoked CICR exhibited little spontaneous activity, whereas dLGN neurons, which do not exhibit LVA Ca^{2+} channel-evoked CICR (Budde et al., 2000), are normally spontaneously active. Although the function of LVA Ca^{2+} channel-evoked CICR in the PVT is unknown, we speculate that this phenomenon may underlie differences in the activity patterns of different thalamic nuclei, particularly during rhythmic burst firing. Such differential coupling of CICR to LVA Ca^{2+} channels may reflect a more generalized functional distinction between specific versus nonspecific thalamocortical signaling pathways.

References

Anderson MP, Mochizuki T, Xie J, Fischler W, Manger JP, Talley EM, Scammell TE, Tonegawa S (2005) Thalamic $Ca_v3.1$ T-type Ca^{2+} channel plays a crucial role in stabilizing sleep. Proc Natl Acad Sci USA 102:1743–1748.

Budde T, Sieg F, Braunewell KH, Gundelfinger ED, Pape HC (2000) Ca^{2+}-induced Ca^{2+} release supports the relay mode of activity in thalamocortical cells. Neuron 26:483–492.

Cui G, Okamoto T, Morikawa H (2004) Spontaneous opening of T-type Ca^{2+} channels contributes to the irregular firing of dopamine neurons in neonatal rats. J Neurosci 24:11079–11087.

Fuentealba P, Timofeev I, Steriade M (2004) Prolonged hyperpolarizing potentials precede spindle oscillations in the thalamic reticular nucleus. Proc Natl Acad Sci USA 101:9816–9821.

Huguenard JR (1996) Low-threshold calcium currents in central nervous system neurons. Annu Rev Physiol 16:329–348.

Lee J, Kim D, Shin HS (2004) Lack of delta waves and sleep disturbances during non-rapid eye movement sleep in mice lacking $\alpha 1_G$-subunit of T-type calcium channels. Proc Natl Acad Sci USA 101:18195–18199.

Paxinos G, Watson C (1998) The rat brain in stereotaxic coordinates, Ed 4. San Diego: Academic.

Perez-Reyes E (2003) Molecular physiology of low-voltage-activated T-type calcium channels. Physiol Rev 83:117–161.

Steriade M, Timofeev I (2003) Neuronal plasticity in thalamocortical networks during sleep and waking oscillations. Neuron 37:563–576.

Tsakiridou E, Bertollini L, de Curtis M, Avanzini G, Pape HC (1995) Selective increase in T-type calcium conductance of reticular thalamic neurons in a rat model of absence epilepsy. J Neurosci 15:3110–3117.